Imaging Science in Dentistry 2022; 52: 375-82
https://doi.org/10.5624/isd.20220051

Correlation between gray values in cone-beam computed tomography and histomorphometric analysis

Najmeh Anbiaee[1], Reihaneh Shafieian[2], Farid Shiezadeh[3], Mohammadtaghi Shakeri[4], Fatemeh Naqipour[5,*]

[1]*Department of Oral and Maxillofacial Radiology, Dental Research Center, School of Dentistry, Mashhad University of Medical Sciences, Mashhad, Iran*
[2]*Department of Anatomy and Cell Biology, School of Medicine, Mashhad University of Medical Sciences, Mashhad, Iran*
[3]*Department of Periodontology, Dental Research Center, School of Dentistry, Mashhad University of Medical Sciences, Mashhad, Iran*
[4]*Department of Community Medicine and Public Health, Mashhad University of Medical Sciences, Mashhad, Iran*
[5]*Department of Oral and Maxillofacial Radiology, Dental Research Center, School of Dentistry, Mashhad University of Medical Sciences, Mashhad, Iran*

ABSTRACT

Purpose: The aim of this study was to analyze the relationships between bone density measurements obtained using cone-beam computed tomography (CBCT) and morphometric parameters of bone determined by histomorphometric analysis.

Materials and Methods: In this *in vivo* study, 30 samples from the maxillary bones of 7 sheep were acquired using a trephine. The bone samples were returned to their original sites, and the sheep heads were imaged using CBCT. On the CBCT images, gray values were calculated. In the histomorphometric analysis, the total bone volume, the trabecular bone volume (referred to simply as bone volume), and the trabecular thickness were assessed.

Results: Statistical testing showed significant correlations between CBCT gray values and total bone volume ($r=0.537$, $P=0.002$), bone volume ($r=0.672$, $P<0.001$), and trabecular thickness ($r=0.692$, $P<0.001$), as determined via the histomorphometric analysis.

Conclusion: The results indicate a significant and acceptable association between CBCT gray values and bone volume, suggesting that CBCT may be used in bone densitometry. ***(Imaging Sci Dent 2022; 52: 375-82)***

KEY WORDS: Cone-Beam Computed Tomography; Densitometry; Bone Density; Histology

Introduction

Cone-beam computed tomography (CBCT) is the most remarkable advancement in maxillofacial imaging since panoramic radiography.[1,2] A primary application of CBCT throughout dentistry is in the relatively noninvasive measurement of bone quality and quantity.[3-5]

Bone quantity is assessed by measuring the length, width, and height of the bone; however, no clear definition and measurement guidelines have yet been established for bone quality evaluation.[2] Bone quality stems from structural (macroscopic and microscopic) and material (modulus of elasticity, mineral density, etc.) properties.[6-8] Materials science explains that the macroscopic properties of materials result from the type, arrangement, and relationship of their microscopic components. In bone, the macroscopic properties, such as shape and density, are determined by the microscopic properties of the bone trabecular meshwork,[9] which is the most homogeneous component of hard tissue and the main anatomical unit of bone function.[8-10] Many methods exist to assess bone quality, including histomorphometric analysis,[11,12] micro-computed tomography (CT),[13-15] CT,[16,17] CBCT,[2] and dual-energy X-ray absorptiometry.[18-20] The most reliable, gold-stan-

All financial resources supporting this study were from the university expenses and for conducting a research project No R.MUMS.DENTISTRY.REC.1398.132.
Received March 10, 2022; Revised July 12, 2022; Accepted July 25, 2022
Published online October 12, 2022
*Correspondence to : Prof. Fatemeh Naqipour
Department of Oral and Maxillofacial Radiology, Dental Research Center, School of Dentistry Mashhad University of Medical Sciences, Mashhad, Iran
Tel) 98-9151811758, E-mail) Naqipour.fn@gmail.com

dard biological system for the microscopic evaluation of bone and the prediction of its biomechanical properties is histomorphometric analysis.[11-13] In this method, secondary to the biological and histological properties, the mechanical features of the bone trabeculae, including the volume, number, and thickness, are evaluated. However, this method is destructive, complex, and time-consuming, and only a few bone sections can be evaluated; therefore, histological analysis cannot serve as a routine bone assessment method.[9,12,21] Micro-CT is a novel gold-standard method for morphometric analysis. Unfortunately, this method can only be used after surgery and is not practical in clinical settings.[22-24] CT is an approved method to quantify bone density and quality by determining the CT number, or Hounsfield units (HU), before surgery. In this imaging technique, radiographic density is numerically determined based on the amount of X-ray absorption by different materials inside the image voxel. The measurements are obtained as gray values (GVs) in CBCT, which are analogous to the use of HUs as a quantitative measure in CT. Although these numbers are not absolute, they can be used to compare the densities of materials. CBCT is a type of CT that is used extensively in dentistry to capture 3-dimensional images. Using CBCT for bone densitometry requires stable, reliable GVs, as well as a constant relationship between these values and density.[1,2] Numerous papers have been published to compare CBCT GVs to HUs. The authors cited limitations including the restricted CBCT field, principles of the basic physics of radiation, and the common limitation of CBCT reconstruction algorithms, where results can depend on the machine type, image acquisition parameters, and the position of the tissue in the field of view (FOV).[25-27]As previously stated, bone quality and density are strongly impacted by the properties of bone trabeculae;[8,9] given the extensive use of CBCT in dentistry, as well as the importance of determining bone quality and quantity, the aim of the present study was to determine the relationship between GVs and data obtained through histomorphometric analysis. A significant correlation between histomorphometric data and GVs would indicate that GVs obtained from CBCT may be used to determine bone density and quality.

Materials and Methods

Sampling

This *in vivo* study was conducted on the maxillary bones of 7 disease-free sheep with approximate ages of 6-12 months, which were considered mature. Sheep were chosen among the available animals because the sheep mandible is similar to the human mandible in format, size, and structure.[28] However, pilot radiographic evaluations indicated that the sheep mandibular bone was very cancellous, with large bone marrow spaces and low trabecular volume. In contrast, the sheep maxillary and palatine bones had an approximately adequate volume of cancellous bone with more uniform trabecular and bone marrow space distribution. After the animals were slaughtered, bone samples from the posterior region of the maxillary palatal process were removed at the Department of Prosthodontics and Implant Dentistry of Mashhad Dental School. Drilling was performed under irrigation at 1000-2000 rpm and a torque of 20-30 N/cm with an 8.0 trephine (1315/8.0, 8.0×9.0 mm; Medesy, Maniago, Italy) (Fig. 1). Then, the samples were placed in their initial sites, the soft palate was sutured in its primary place, and the sheep's heads were fixed. In this step, 50 bone samples were acquired.

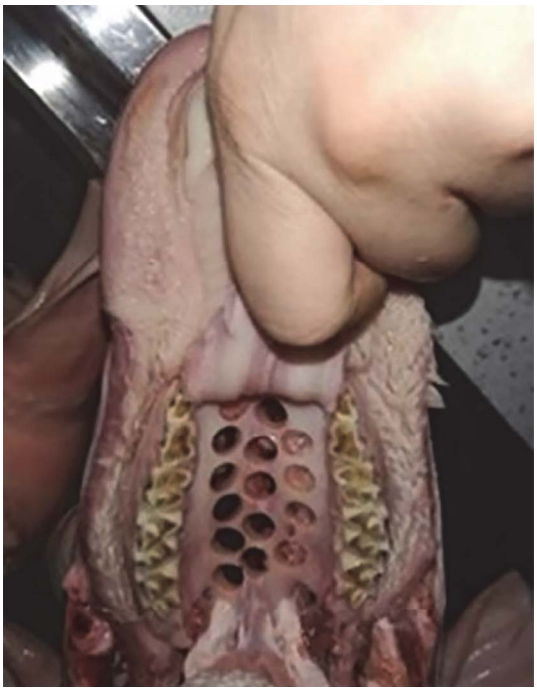

Fig. 1. Removal of a sheep's palate bone with a trephine.

Preparation and evaluation of CBCT images

Imaging was conducted using a CBCT unit (ProMax 3D Max; Planmeca, Helsinki, Finland) with a FOV of 10×10 cm and standard exposure conditions (90 kVp and 12 mA) (Fig. 2). Romexis Viewer software (v3.8.3.R; Planmeca) was used for deriving GVs to evaluate the bone density. Because the bone specimens were acquired with the trephine and then returned to their original locations, their

Fig. 2. Sheep's head fixation and preparation for image acquisition.

sidewalls were visible and traceable on the CBCT images. To analyze the images, using the Romexis software, the explorer tool was selected on the first page. Then, from the left menu, the settings option was opened and the following were selected: axial line, sagittal line, coronal line, and rulers. On the sagittal and coronal sections, the bone samples were moved to align the sidewalls of the target cylinder parallel to the sagittal and coronal lines. Thus, the cross-sections of all specimens in both sagittal and coronal views were parallel to the axial line, and correspondingly, the removed cylindrical specimen was placed perpendicular to the axial plane. The sections observed in the axial view were therefore adjusted similarly to the section of the histological incision. Next, on the same page, in the left menu and the Annotations section, the "Measure Cube" option was selected. Using this option in the axial view, a shape with a length and width of 5 × 5 mm and a fixed height of 2 mm was drawn inside the desired cylinders, without considering the cortical bone of the alveolar crest area, and immediately afterward, in the spongy bone area. The dimensions of the shape were similarly determined and fixed in the sagittal and coronal views (Fig. 3).

As shown in Figure 3, the software measures and displays several values. "Vol" is the volume of the selected shape, and "w," "h," and "d" represent its width, length, and height, respectively. "Avg" indicates the CBCT GVs measured by the software that are indicative of density. "StD" represents the standard deviation, while "R" indicates the range of the densities measured in the selected area. In this step, any sample without a complete cross-section or with a height less than 2 mm was excluded.

Histological preparation and histomorphometric analysis

Specimens were fixed in 10% buffered formalin for 3 days and decalcified using 10% ethylenediaminetetraacetic acid (pH 7.2) for the following 4 weeks. Afterward, similar to the procedure for the CBCT images, the cortical bone (1 mm of the external surface of the palate) was removed, and a 2-mm-tall segment of the cylindrical bone was used as the final sample. In brief, tissue preparation of the samples was performed in the following order: dehydration with increasing concentrations of ethanol, clarification with xylene, immersion in paraffin, and serial sectioning of the paraffin molds by microtome into 6-μm sections. Finally, the tissues were stained with hematoxylin and eosin and observed under an optical microscope (BX51; Olympus, Tokyo, Japan). Some cross-sections were randomly photographed with a camera (IXUS 950 IS; Canon, Tokyo, Japan) attached to the microscope (Fig. 4). Within these sections, the total bone volume (TBV; the sum of the bone trabeculae and bone marrow spaces), the trabecular bone volume (referred to as bone volume [BV]), and the trabecular thickness (Tb.Th) were calculated with the Cavalieri principle using ImageJ verified stereological software (available at https://imagej.nih.gov/ij/). Ultimately, 30 samples were confirmed for histomorphometric analysis, and the associations of CBCT GVs with TBV, BV, and Tb.Th were measured.

Statistical analysis

The distribution of data was analyzed using the Kolmogorov-Smirnov test. Pearson analysis was conducted to calculate the correlation coefficients (r values) between variables. A linear regression test was used to predict GVs based on histomorphometric data and to determine the formula relating GV and BV values. *P*-values less than 0.05 were considered to indicate statistical significance, as set in SPSS Statistics 17.0.0 (SPSS Inc., Chicago, IL, USA) software.

Results

Table 1 shows the average, minimum, maximum, and

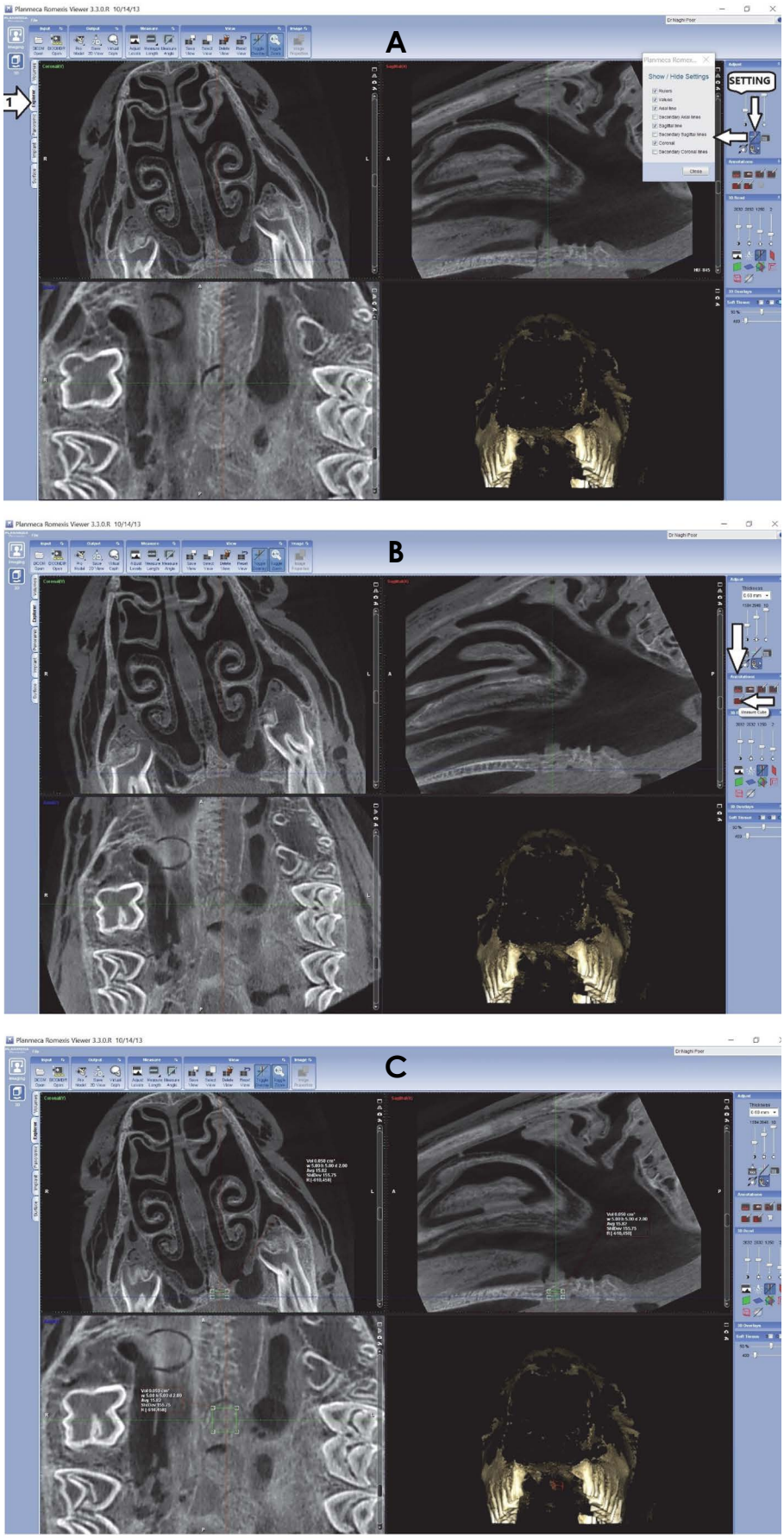

Fig. 3. A. In the Explorer menu of Planmeca Romexis software, the settings option is selected and "Rulers," "Axial line," "Sagittal line," and "Coronal line" are activated as displayed arrows. Then, the sample is positioned parallel in the axial view with rotation of the images in the coronal and sagittal views. B. In the annotations menu, the user chooses "Measure Cube." C. A shape is drawn (5 × 5 × 2 mm) in the axial view, and then 5 mm × 5 mm is set for length and width and 2 mm for height in the coronal and sagittal views.

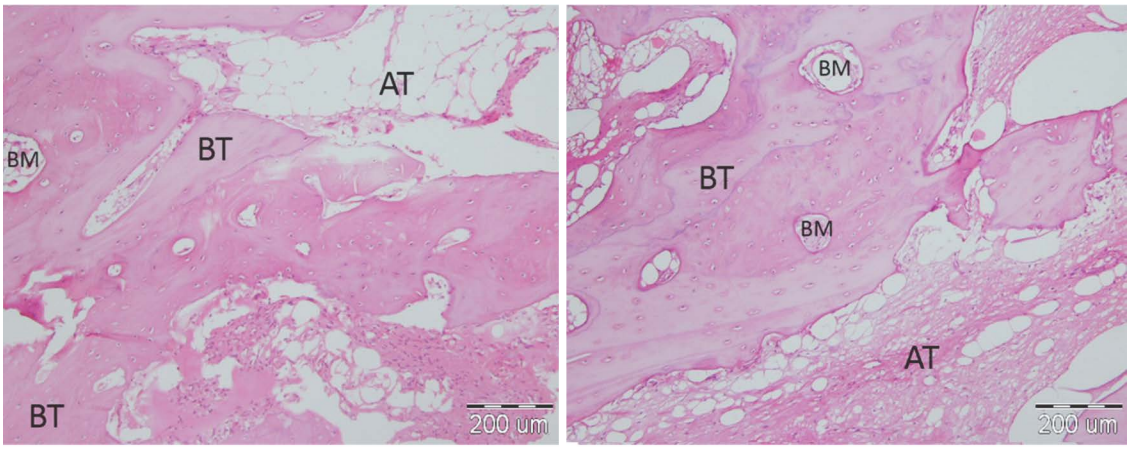

Fig. 4. Histological photographs obtained from the experimental animals show the bone tissues including bone marrow spaces (BM), bone trabeculae (BT), and adipose tissue (AT) (H&E stain, original magnification ×400).

Table 1. Comparison of variables

Variables	Number	Average	Standard deviation	Minimum	Maximum
TBV	30	28.56	11.85	9.22	58.78
BV	30	16.83	9.58	3.78	40.65
Tb.Th	30	3.39	1.89	0.73	8.13
GVs	30	155.30	123.18	−63.37	466.53

TBV: total bone volume, BV: bone volume (trabecular bone volume), Tb.Th: trabecular thickness, GVs: gray values.

Table 2. Association between variables using Pearson correlation analysis

		TBV	BV	Tb.Th
GVs	Pearson correlation	0.537*	0.672*	0.692*
	Sig. (2-tailed)	0.002	$P<0.001$	$P<0.001$

TBV: total bone volume, BV: bone volume (trabecular bone volume), Tb.Th: trabecular thickness, GVs: gray values.

Table 3. Association between variables using linear regression analysis

Variables	*P*-value	R	R squared
TBV and GVs	0.002	0.537	0.288
BV and GVs	0	0.672	0.452
Tb.Th and GVs	0	0.692	0.479

TBV: total bone volume, BV: bone volume (trabecular bone volume), Tb.Th: trabecular thickness, GVs: gray values.

standard deviation values for TBV, BV, Tb.Th, and GV for the 30 samples. The results of the Kolmogorov-Smirnov test indicated a normal distribution of data. The associations between variables based on the Pearson correlation test and linear regression analysis are shown in Tables 2 and 3, respectively. The GVs were significantly associated with TBV ($P=0.002$), BV ($P<0.001$), and Tb.Th ($P<0.001$). The correlation coefficients (r) between GVs and the 3 histomorphometric measurements (TBV, r=0.537; BV, r=0.672; Tb.Th, r=0.692) were also obtained. Based on regression analysis, the relationship between GVs and BV was characterized by the following formula: GV = 9.879 + 8.642 × BV.

Discussion

Despite the many existing studies on the reliability of GVs obtained with CBCT, the usefulness of these values in determining the bone mineral density (BMD) has been questionable. For example, some studies have shown a linear relationship between GVs and the BMD obtained from dual-energy X-ray absorptiometry,[18,20,29] and others have shown a significant correlation between CBCT and micro-CT in the evaluation of bone quality.[30-32] Recent stud-

ies have indicated a linear relationship between the GVs obtained with CBCT and the HUs obtained with CT.[2,26,30] However, different beam geometry, scattered X-rays, and the effect of beam hardening on CBCT imaging have been shown to cause inconsistent, uncoordinated, and arbitrary GVs in CBCT, so these values could not be used to indicate the density of bone structures as HU values can be used in CT. Many factors affect the GVs obtained from CBCT, including variations among devices,[33,34] in the dimensions of the FOV,[27,35,36] and in the position of the object within the FOV,[37] among others. As previously shown in studies utilizing a relatively small FOV, by reducing scattered radiation and resulting artifacts, less noise and more contrast are obtained; consequently, the density derived from CBCT imagery becomes more reliable with increasing image quality.[1,2,27] Therefore, in the present study, a medium FOV (10 cm × 10 cm) was chosen to allow for the use of the smallest possible field by fully displaying the desired image in a single field.

Recent studies have shown that objects in the center of the field are less affected by radiation geometry and artifacts than those on the outskirts.[2,37] The presence of external and internal masses has also been found to adversely impact GVs.[38] Thus, in this study, the masses in the center of the FOV were extracted (i.e., the palate and nasal septum). As such, a uniform structure of the bone was obtained, and due to the use of animal samples, metal artifacts caused by dental restorations were not a concern. The present study obtained acceptable and significant associations between GVs and TBV ($P=0.002$), BV ($P<0.001$), and Tb.Th ($P<0.001$). The correlation coefficients between GVs and TBV ($r=0.537$), BV ($r=0.672$), and Tb.Th ($r=0.692$) were also determined. As shown, the coefficients for BV and Tb.Th are similar. The difference between these values and the lower coefficient for TBV could be due to the presence of various soft tissues (red bone marrow, salivary glands, adipose tissue, etc.) inside the bone marrow space. Each tissue type has its own attenuation coefficient, with adipose tissue having a particularly low density that could result in a negative tissue density reading. Therefore, it seems that more accurate GVs are obtained in bone trabeculae with a known and uniform density than in those with a non-uniform density.

On a digital radiography image, the density of each pixel is directly associated with the atomic number and density of the tissue material. Given that soft tissue has a lower atomic number and density than hard tissue, the presence of scattered radiation could severely impact the final density value for each pixel of soft tissue; in contrast, the hard tissue of bone has a higher atomic number and density, so scattered radiation and noise have a smaller effect on the total density of hard tissue pixels. Accordingly, the present study results show a stronger association between GVs and BV than between GVs and TBV.

Another reason for this claim is the large span of GVs, which is represented by Romexis software as R (range) and includes a wide range of negative to positive numbers. Romexis software data showed that the examined tissue was completely heterogeneous with regard to gray values. The correlation coefficient of GVs with Tb.Th confirmed this finding ($r=0.692$ and $P<0.001$). Trabecular thickness has a relatively strong association with GVs. Therefore, CBCT is reliable in determining the density of materials, which is dependent on their atomic number and density.

In a study by Todisco and Trisi,[16] the researchers compared the HUs from CT imagery with histomorphometric measurements and found a significant correlation between CT HUs and BV ($r=0.691$). This coefficient is very similar to that found in the present study, and given that using HUs is an accepted protocol in bone densitometry, using GVs may also be reliable in densitometry.

Notably, many studies have included the use of micro-CT to evaluate the accuracy of GVs and morphometric analysis data, and only a few have compared these values with histomorphometric findings. Due to the accessibility of histomorphometric analysis, this method was used in the present study.

While histomorphometric analysis and micro-CT are both gold standards for evaluating bone morphometric parameters, it is impossible to observe and evaluate soft tissues with micro-CT at the level seen under microscope. For example, TBV, which includes bone trabeculae and the bone marrow space, cannot be assessed on micro-CT.

Numerous studies have been conducted to examine the association between BV/TV (total volume) and GVs. The examined volume in the present study was 100 mm^3 for all samples; therefore, the BV/TV ratio in the present study was referred to simply as BV.

Parsa et al.[30] found a strong association between GVs and BV/TV using micro-CT ($r=0.82$) in an *in vitro* study on the human cadaver mandible. Moreover, the results indicated a high correlation between HUs and micro-CT BV/TV ($r=0.91$). The researchers also reported a strong association between GVs and HUs. Monje et al.[31] found a correlation of $r=0.769$ between GVs and BV/TV in micro-CT, which is indicative of a strong association between these variables.

A significant association was also present between GVs and Tb.Th (r = 0.491). Similarly, a strong association between GVs and micro-CT BV/TV (r = 0.835) was found in a study by Wang et al.[32] They also found a correlation between GVs and Tb.Th (r = 0.138). Monje et al.[31] studied the posterior maxilla, and Wang et al.[32] studied the posterior mandible, both in humans. In another study, González-García and Monje[22] obtained correlations between GVs and BV/TV (r = 0.858) and Tb.Th (r = 0.574) in micro-CT.

Given the results of these studies and the present research, a strong association between GVs and BV/TV can be inferred. However, the correlation coefficients (r) in the present study were slightly lower than in other studies,[22,30-32] perhaps due to different histomorphometric and micro-CT methods.

In the present study, the sample was obtained from sheep bone, which has larger bone marrow spaces than human bone tissue. The histomorphometric analysis indicated a mean BV of 16.82%, which was smaller than the values found in previous studies. The mean BV/TV values in the studies by González-García and Monje,[22] Todisco and Trisi,[16] Parsa et al.,[30] and Monje et al.[31] were 48.7%, 45.624%, 32.35%, and 31.42%, respectively. These results indicate a low percentage of bone tissue in sheep bone in comparison to human samples.

Notably, in most of those prior studies, the bone samples were acquired using a 2.0 trephine. The present authors have frequently observed that in both human and animal samples, using a 2.0 trephine compresses the bony trabeculae, reducing the bone marrow spaces and increasing the trabecular density during sampling. Therefore, the present animal study was conducted using a larger trephine (8 mm).

In a literature review, Suttapreyasri et al.[12] showed a strong association between cortical bone thickness and BV/TV; however, they found no statistically significant association between BV/TV and GVs. A FOV of 40 mm × 40 mm and a CBCT Accuitomo device (Morita, Kyoto, Japan) were used in that study. Corpas Ldos et al.[39] did not report a correlation between GVs and histomorphometric analysis of the peri-implant bone. Apparently, they did not consider the issue of implant metal artifacts—which can considerably impact GVs—in that study.

In conclusion, in the present study, a significant correlation was found between GVs and BV. Additionally, the results indicate that GV values obtained from CBCT are more strongly associated with bone tissue alone than with soft tissue in bone marrow spaces considered alongside bone.

Acknowledgments

These authors thank Mashhad University of Medical Sciences for the support.

Conflicts of Interest: None

References

1. Scarfe WC, Li Z, Aboelmaaty W, Scott SA, Farman AG. Maxillofacial cone beam computed tomography: essence, elements and steps to interpretation. Aust Dent J 2012; 57 Suppl 1: 46-60.
2. Pauwels R, Jacobs R, Singer SR, Mupparapu M. CBCT-based bone quality assessment: are Hounsfield units applicable? Dentomaxillofac Radiol 2015; 44: 20140238.
3. Shukla S, Chug A, Afrashtehfar KI. Role of cone beam computed tomography in diagnosis and treatment planning in dentistry: an update. J Int Soc Prev Community Dent 2017; 7(Suppl 3): S125-36.
4. Weiss R 2nd, Read-Fuller A. Cone beam computed tomography in oral and maxillofacial surgery: an evidence-based review. Dent J (Basel) 2019; 7: 52.
5. Chrcanovic BR, Albrektsson T, Wennerberg A. Bone quality and quantity and dental implant failure: a systematic review and meta-analysis. Int J Prosthodont 2017; 30: 219-37.
6. Bilhan H, Arat S, Geckili O. How precise is dental volumetric tomography in the prediction of bone density? Int J Dent 2012; 2012: 348908.
7. Kuroshima S, Kaku M, Ishimoto T, Sasaki M, Nakano T, Sawase T. A paradigm shift for bone quality in dentistry: a literature review. J Prosthodont Res 2017; 61: 353-62.
8. He RT, Tu MG, Huang HL, Tsai MT, Wu J, Hsu JT. Improving the prediction of the trabecular bone microarchitectural parameters using dental cone-beam computed tomography. BMC Med Imaging 2019; 19: 10.
9. Jindal M, Lakhwani O, Kapoor S, Chandoke R, Kaur O, Arora B, et al. Correlation between bone histomorphometry and bone strength. Trop J Med Res 2017; 20: 25.
10. David O, Leretter M, Neagu A. The quality of trabecular bone assessed using cone-beam computed tomography. Rom J Biophys 2014; 24: 227-41.
11. Rokn AR, Labibzadeh A, Ghohroudi AA, Shamshiri AR, Solhjoo S. Histomorphometric analysis of bone density in relation to tactile sense of the surgeon during dental implant placement. Open Dent J 2018; 12: 46-52.
12. Suttapreyasri S, Suapear P, Leepong N. The accuracy of cone-beam computed tomography for evaluating bone density and cortical bone thickness at the implant site: micro-computed tomography and histologic analysis. J Craniofac Surg 2018; 29: 2026-31.
13. Kivovics M, Szabó BT, Németh O, Iványi D, Trimmel B, Szmirnova I, et al. Comparison between micro-computed tomography and cone-beam computed tomography in the assessment of bone quality and a long-term volumetric study of the augment-

ed sinus grafted with an albumin impregnated allograft. J Clin Med 2020; 9: 303.
14. Panmekiate S, Ngonphloy N, Charoenkarn T, Faruangsaeng T, Pauwels R. Comparison of mandibular bone microarchitecture between micro-CT and CBCT images. Dentomaxillofac Radiol 2015; 44: 20140322.
15. Kulah K, Gulsahi A, Kamburoğlu K, Geneci F, Ocak M, Celik HH, et al. Evaluation of maxillary trabecular microstructure as an indicator of implant stability by using 2 cone beam computed tomography systems and micro-computed tomography. Oral Surg Oral Med Oral Pathol Oral Radiol 2019; 127: 247-56.
16. Todisco M, Trisi P. Bone mineral density and bone histomorphometry are statistically related. Int J Oral Maxillofac Implants 2005; 20: 898-904.
17. Selvaraj A, Jain RK, Nagi R, Balasubramaniam A. Correlation between gray values of cone-beam computed tomograms and Hounsfield units of computed tomograms: a systematic review and meta-analysis. Imaging Sci Dent 2022; 52: 133-40.
18. Sghaireen MG, Ganji KK, Alam MK, Srivastava KC, Shrivastava D, Rahman SA, et al. Comparing the diagnostic accuracy of CBCT grayscale values with DXA values for the detection of osteoporosis. Appl Sci (Basel) 2020; 10: 4584.
19. Payahoo S, Jabbari G. The ability of cone beam computed tomography to predict osteopenia and osteoporosis via radiographic density derived from cervical vertebrae. Int J Sci Res Dent Med Sci 2019; 1: 18-22.
20. Shokri A, Ghanbari M, Maleki FH, Ramezani L, Amini P, Tapak L. Relationship of gray values in cone beam computed tomography and bone mineral density obtained by dual energy X-ray absorptiometry. Oral Surg Oral Med Oral Pathol Oral Radiol 2019; 128: 319-31.
21. Kim DG. Can dental cone beam computed tomography assess bone mineral density? J Bone Metab 2014; 21: 117-26.
22. González-García R, Monje F. The reliability of cone-beam computed tomography to assess bone density at dental implant recipient sites: a histomorphometric analysis by micro-CT. Clin Oral Implants Res 2013; 24: 871-9.
23. Kang SR, Bok SC, Choi SC, Lee SS, Heo MS, Huh KH, et al. The relationship between dental implant stability and trabecular bone structure using cone-beam computed tomography. J Periodontal Implant Sci 2016; 46: 116-27.
24. Liang X, Zhang Z, Gu J, Wang Z, Vandenberghe B, Jacobs R, et al. Comparison of micro-CT and cone beam CT on the feasibility of assessing trabecular structures in mandibular condyle. Dentomaxillofac Radiol 2017; 46: 20160435.
25. Mehralizadeh S, Talaipour AR, Olyaee P, Amiri Siavoshani M. Correlation between tissue densities in computed tomography and three different cone-beam computed tomography units (in vitro). J Res Dent Maxillofac Sci 2020; 5: 13-20.
26. Razi T, Niknami M, Alavi Ghazani F. Relationship between Hounsfield unit in CT scan and gray scale in CBCT. J Dent Res Dent Clin Dent Prospects 2014; 8: 107-10.
27. Shokri A, Ramezani L, Bidgoli M, Akbarzadeh M, Ghazikhanlu-Sani K, Fallahi-Sichani H. Effect of field-of-view size on gray values derived from cone-beam computed tomography compared with the Hounsfield unit values from multidetector computed tomography scans. Imaging Sci Dent 2018; 48: 31-9.
28. Khojastepour L, Mohammadzadeh S, Jazayeri M, Omidi M. In vitro evaluation of the relationship between gray scales in digital intraoral radiographs and Hounsfield units in CT scans. J Biomed Phys Eng 2017; 7: 289-98.
29. Guerra EN, Almeida FT, Bezerra FV, Figueiredo PT, Silva MA, De Luca Canto G, et al. Capability of CBCT to identify patients with low bone mineral density: a systematic review. Dentomaxillofac Radiol 2017; 46: 20160475.
30. Parsa A, Ibrahim N, Hassan B, van der Stelt P, Wismeijer D. Bone quality evaluation at dental implant site using multislice CT, micro-CT, and cone beam CT. Clin Oral Implants Res 2015; 26: e1-7.
31. Monje A, Monje F, González-García R, Galindo-Moreno P, Rodriguez-Salvanes F, Wang HL. Comparison between microcomputed tomography and cone-beam computed tomography radiologic bone to assess atrophic posterior maxilla density and microarchitecture. Clin Oral Implants Res 2014; 25: 723-8.
32. Wang F, Huang W, Wu Y, Montanero-Fernandez J, Sheridan RA, Wang HL, et al. Accuracy of cone beam computed tomography grayscale density in determining bone architecture in the posterior mandible: an in vivo study with microcomputed tomography validation. Int J Oral Maxillofac Implants 2017; 32: 1074-9.
33. Van Dessel J, Nicolielo LF, Huang Y, Slagmolen P, Politis C, Lambrichts I, et al. Quantification of bone quality using different cone beam computed tomography devices: accuracy assessment for edentulous human mandibles. Eur J Oral Implantol 2016; 9: 411-24.
34. England GM, Moon ES, Roth J, Deguchi T, Firestone AR, Beck FM, et al. Conditions and calibration to obtain comparable grey values between different clinical cone beam computed tomography scanners. Dentomaxillofac Radiol 2017; 46: 20160322.
35. Oliveira ML, Tosoni GM, Lindsey DH, Mendoza K, Tetradis S, Mallya SM. Assessment of CT numbers in limited and medium field-of-view scans taken using Accuitomo 170 and Veraviewepocs 3De cone-beam computed tomography scanners. Imaging Sci Dent 2014; 44: 279-85.
36. Rodrigues AF, Campos MJ, Chaoubah A, Fraga MR, Farinazzo Vitral RW. Use of gray values in CBCT and MSCT images for determination of density: influence of variation of FOV size. Implant Dent 2015; 24: 155-9.
37. Lindfors N, Lund H, Johansson H, Ekestubbe A. Influence of patient position and other inherent factors on image quality in two different cone beam computed tomography (CBCT) devices. Eur J Radiol Open 2017; 4: 132-7.
38. Candemil AP, Salmon B, Freitas DQ, Ambrosano GM, Haiter-Neto F, Oliveira ML. Metallic materials in the exomass impair cone-beam CT voxel values. Dentomaxillofac Radiol 2018; 47: 20180011.
39. Corpas Ldos S, Jacobs R, Quirynen M, Huang Y, Naert I, Duyck J. Peri-implant bone tissue assessment by comparing the outcome of intra-oral radiograph and cone beam computed tomography analyses to the histological standard. Clin Oral Implants Res 2011; 22: 492-9.